New ethenzamide-trimesic acid cocrystal: Equilibrium solubility

Shuting Lin
Zhejiang University of Science and Technology
Yingfan Xia
Zhejiang University of Science and Technology
Jiarong Zhang
Zhejiang University of Science and Technology
Weijie Sun
Zhejiang University of Science and Technology
Xinxin Xu
Zhejiang University of Science and Technology
Xiaoyu Jin
Zhejiang University of Science and Technology
Penghui Ren
Zhejiang University of Science and Technology
Jiayi Jiang
Zhejiang University of Science and Technology
Chengjun Jiang (jcj312@zust.edu.cn)
Zhejiang University of Science and Technology

Research Article

Keywords: Pharmaceutical cocrystal, Ethenzamide, Crystal engineering, Solubility

Posted Date: January 9th, 2023

DOI: https://doi.org/10.21203/rs.3.rs-2396758/v1

Abstract

To study the influence of drug cocrystal on the solubility of active pharmaceutical ingredients (APIs). The ETZ·2TMA·MeOH cocrystal was obtained by the solution evaporation crystallization method. The cocrystal structure was characterized by Single Crystal X-ray Diffractometer. The single crystal belongs to orthorhombic crystal system with space group $P2_12_12_1$(no.19), a = 12.9863(9) Å, b = 16.6603(11) Å, c = 25.9260(16) Å, V = 5609.2(6) $Å^3$, Z = 8, T = 170.00 K. The main forces are the formation of intermolecular hydrogen bonds between the amide groups on ETZ and the carboxyl groups on TMA and the hydroxyl group on methanol. In addition, the solubility of ETZ and ETZ·2TMA·MeOH cocrystal was determined. The results show that, in contrast to most cocrystal systems that improve solubility, the solubility of ETZ·2TMA·MeOH decreased to 19.30 % of pure ETZ.

1 Introduction

Ethenzamide (CAS: 938-73-8, 2-ethoxybenzamide, ETZ) is a non-steroidal anti-inflammatory drug with analgesic and antipyretic effects[1]. It can be used to treat mild to moderate pain in muscle, bone and joint diseases. ETZ belongs to class II of Biological drug Classification System (BCS), and its main disadvantages are poor solubility and low bioavailability[2]. The structures of cocrystal of ETZ have been published and deposited in CSD (Cambridge Structural Database), which was obtained with furosemide (CCDC:2114160, SARQOV)[3], sinapic acid (CCDC:1581650, DEYQUW)[4], 2,5-dihydroxybenzoic acid (CCDC:1522933, FENQEX), 3,4-dihydroxybenzoic acid (CCDC:1522937, FENRIC)[5], phenol (CCDC:1879336, VUKSEC)[6], 3,5-dinitrobenzoic acid (CCDC:752467, WUZHOP)[7], 2,4-dihydroxybenzoic acid (CCDC:1825011, JIFHAK)[8], 3,4,5-trihydroxybenzoic acid (CCDC:1468148, ORIKIL), 2-nitrobenzoic acid (CCDC:1468153, ORIKOR), 3-nitrobenzoic acid (CCDC:1468154, ORIKUX), 2,4-dinitrobenzoic acid (CCDC:1468159, ORILAE), 3-methylbenzoic acid (CCDC:1468161, ORILEI)[9], 2-hydroxybenzoic acid (CCDC:752480, REHSAA)[10], pentanedioic acid (CCDC:1854255, TIWPIB)[11], (2Z)-but-2-enedioic acid (CCDC:1854256, TIWPOH)[11], Flufenamic Acid (CCDC:1448786, FAQXAZ)[12], Ferulic acid (CCDC:1448786, FAQXAZ)[13], propanedioic acid (CCDC:1854257, TIWPUN)[14], ethylmalonic acid (CCDC:752465, VAKTOS)[15], Saccharin (CCDC:711674, VUHFIO)[16]and so on.

Different coformers can cause different trend of solubilities. For example, ETZ·3,5-dinitrobenzoic acid (19.47 $mg·mL^{-1}$), ETZ·2,4-dihydroxybenzoic acid (4.78 $mg·mL^{-1}$) improved the solubility of ETZ (1.45 $mg·mL^{-1}$), while ETZ·ferulic acid (1.15 $mg·mL^{-1}$) reduced the solubility of ETZ (1.45 $mg·mL^{-1}$). In this research, we discovered the cocrystal of ETZ·2TMA·MeOH, which laid a foundation for the further study of ETZ new cocrystal.

2 Experimental

2.1 Materials

Ethenzamide and Trimesic acid were purchased from Energy Chemical Co., Ltd. Analytical grade solvents were used for the crystallization experiments. All purchased from Shanghai Lingfeng Chemical Reagent Co., Ltd.

2.2 Cocrystal Growth

Equimolar quantities of ETZ (0.20 mol) and TMA (0.20 mol) were added to a mixed solvent of 2 mL of methanol and 3 mL of toluene in a 10 mL glass vial. The slurry was stirred at 60°C for 10 min. The obtained clear solution was cooled down slowly to the room temperature for 2 days.

2.3 Fourier transform-infrared spectroscopy (FT-IR)

The infrared spectra of samples were evaluated by an FT-IR spectrometer (Bruker Alpha FT-IR spectrometer). The measurements were performed in a range of 4000 – 400 cm^{-1} with a resolution of 4 cm^{-1}. Powder samples (about 2 mg) were manually mixed with 100 mg of dry KBr in an agate mortar and pressed into thin pellets. Data were analyzed by Spectrum software.

2.4 Powder X-Ray diffraction (PXRD)

The diffraction patterns were measured on Rigaku Ultima IV X-ray Diffractometer (Rigaku, Tokyo, Japan) using Cu Kα X-ray (λ = 1.5406 Å) and the generator operated at 40 kV and 40 mA. The scans ran from 5.0 ° to 50.0 ° (2θ), with an increasing step size of 0.02 ° and the scan rate of 5 °·min^{-1}.

2.5 Single Crystal X-Ray diffraction(SXRD)

A single crystal of suitable size and good quality was measured by using an area detector on a Bruker APEX-II CCD diffractometer with graphite monochromatic Ga-Kα radiation (λ = 1.34138 Å). Absorption corrections were applied by using multi-scan program. Using Olex2, the structure was solved with the ShelXT structure solution program using Intrinsic Phasing and refined with the ShelXL refinement package using Least Squares minimisation.

2.6 Solubility and Dissolution studies

The dissolution studies of ETZ and ETA·2TMA·MeOH were measured by using equal molar samples at 37 ^{o}C for oscillation. Aliquots of 1 mL were withdrawn at predetermined time points (5, 10, 15, 30, 45, 60, 120, 180, 240 and 1380 min) substituting the same with equal quantity of fresh dissolution media.

The solubility and dissolution rate of ETZ and ETA·2TMA·MeOH were quantified by High Performance Liquid Chromatography. An Waters e2695 series HPLC equipped with a UV detector (2489) and an automated injector. Methanol-water (80: 20) were used as mobile phase at a flow rate of 1 mL/min in an isocratic mode on an Agilent Zorbax SB-C18 (4.6 mm × 250 mm, 5 µm) column at 25°C. After suitable dilution, 10 µL of sample was injected, and the absorbance of elute was recorded at 235 nm.

2.7 Hirshfeld surface analysis

Both the Hirshfeld surface image and 2D fingerprint are generated by Crystal Explorer software.

3 Results And Discussion

3.1 Solid State XRay Crystal Structure analysis

Table 1
ETA·2TMA·MeOH cocrystal crystallography and refinement data

	ETZ·2TMA·MeOH
Empirical formula	$C_{28}H_{27}NO_{15}$
Formula weight	617.50
Temperature / K	170.00
Crystal system	orthorhombic
Space group	$P2_12_12_1$
a/Å	12.9863(9)
b/Å	16.6603(11)
c/Å	25.9260(16)
α/°	90
β/°	90
γ/°	90
Volume/$Å^3$	5609.2(6)
Z	8
$\rho_{calc}g/cm^3$	1.462
μ/mm^1	0.660
F(000)	2576.0
Crystal size/mm^3	0.08 × 0.06 × 0.03
Radiation	GaKα (λ = 1.34138)
2Θ range for data collection/°	5.486 to 114.53
Index ranges	$-16 \leq h \leq 15$, $-20 \leq k \leq 20$, $-31 \leq l \leq 32$
Reflections collected	42349
Independent reflections	11301 [R_{int} = 0.0518, R_{sigma} = 0.0557]
Data / restraints / parameters	11301/7/821
Goodness-of-fit on F^2	1.044
Final R indexes [I >= 2σ (I)]	R_1 = 0.0525, wR_2 = 0.1223

	ETZ·2TMA·MeOH
Final R indexes [all data]	R_1 = 0.0900, wR_2 = 0.1462
Largest diff. peak/hole / e $Å^{-3}$	0.21/-0.31
Flack parameter	0.03(11)

The ETZ·2TMA·MeOH cocrystal was obtained from mixed solvent of methanol and toluene at room temperature by solvent evaporation method. The single crystal belongs to orthorhombic crystal system with space group $P2_12_12_1$ (Table 1).. In the unit cell of cocrystal, the main forces are the formation of intermolecular hydrogen bonds between the amide groups on ETZ and the carboxyl groups on TMA and the hydroxyl group on methanol (Fig. 1, Table 2). On the one hand, the O atom on the amide group of the ETZ molecule is a hydrogen bond acceptor, and the H atom on the carboxyl group (O-H) of the TMA molecule is a hydrogen bond donor, forming an intermolecular hydrogen bond O-H…O (symmetry code: +X, +Y, -1 + Z) [length 2.523(4) Å, angle 165.4 °]. On the other hand, the O atom on the hydroxyl group of methanol molecule is a hydrogen bond acceptor, the H atom on the molecular carboxyl group (O-H) of the ETZ molecule is a hydrogen bond donor, forming an intermolecular hydrogen bond O-H…O (symmetry code: +X, +Y, -1 + Z) [length 2.515(4) Å, angle 170.2 °]. The methanolate cocrystal of ETZ and TMA were formed. Views of the calculated ETA·2TMA·MeOH Hirshfeld surface and 2D fingerprint were shown in Fig. 2. The force of H... O/O... H is 34.5%, and the force of H... N/N... H is 0.7%. The force of hydrogen bond between ETZ and TMA mainly depends on H... O/O... H force.

Table 2
ETA·2TMA·MeOH cocrystalline hydrogen bonds

D	H	A	d(D-H)/Å	d(H-A)/Å	d(D-A)/Å	D-H-A/°
N1	H1B	O2	0.88	1.97	2.654(4)	133.5
O3	H3A	O1	0.84	1.70	2.523(4)	165.4
O5	H5A	O29	0.84	1.68	2.515(4)	170.2
O8	H8	$O24^{1}$	0.84	1.89	2.725(4)	172.1
O11	H11	$O26^{2}$	0.84	1.85	2.664(4)	161.3
O20	H20	$O6^{3}$	0.84	1.82	2.636(4)	162.9
N2	H2B	O22	0.88	1.98	2.663(5)	133.0
O23	H23A	O21	0.84	1.69	2.511(4)	165.0
O25	H25A	O30	0.84	1.68	2.510(4)	171.6
O28	H28	$O4^{1}$	0.84	1.91	2.739(4)	171.0
O30	H30A	$O12^{4}$	0.84	1.82	2.655(4)	171.6
O10	H10	$O17^{5}$	0.87(3)	1.81(3)	2.674(4)	171(9)
O13	H13	O15	0.88(3)	1.73(3)	2.596(4)	172(8)
O16	H16A	O14	0.86(3)	1.82(3)	2.662(4)	165(8)
O18	H18	$O9^{6}$	0.87(3)	1.72(3)	2.590(4)	177(9)
O29	H29	$O19^{1}$	0.87(3)	1.79(3)	2.644(4)	168(7)

^{1}1-X,-1/2 + Y,-1/2-Z; ^{2}+X,+Y,1 + Z; ^{3}1-X,1/2 + Y,-1/2-Z; ^{4}+X,+Y,-1 + Z; ^{5}+X,-1 + Y,+Z; ^{6}+X,1 + Y,+Z

3.2 PXRD analysis

The crystal structures of ETZ, TMA, and ETA·2TMA·MeOH were measured by PXRD (Fig. 3). The peaks at 2θ = 9.64 °, 14.54 °, 14.70 °, 19.36 °, 25.32 °, and 33.78 °, which are the characteristic peaks of ETZ, disappeared in the PXRD result of ETA·2TMA·MeOH. Meanwhile, a number of new peaks belonging to ETA·2TMA·MeOH emerged at 2θ = 26.84 °. Thus, the formation of ETA·2TMA·MeOH can be confirmed by the notable changes through the PXRD.

3.4 FT-IR analysis

The synthesized ETA·2TMA·MeOH was analyzed by FT-IR spectroscopy. FT-IR spectra of ETZ, TMA and ETA·2TMA·MeOH were compared in order to confirm the cocrystal formation. All the molecular cocrystals exhibited a change in carbonyl stretching frequency of acid group with respect to their starting material.

In the ETA·2TMA·MeOH, significant shift of carboxylate (–C = O) and amino ($–NH_2$) stretching vibration was observed (Fig. 4). The characteristic peak of N-H in the molecular structure of ETZ was shift from 3370.51 cm^{-1} to 3453.93 cm^{-1}, the characteristic absorption peak of C = O in the molecular structure of TMA was shift from 1644.27 cm^{-1} to 1705.51 cm^{-1}.

3.5 Solubility study

It is well known that the solid form of APIs has a substantial impact on the solubility and dissolution profiles of drug. Therefore, it is important to select an appropriate API solid state forms for successful drug development. According to the Biopharmaceutical Classification System (BCS), ETZ was classified as a low solubility drug (BCS class). Solubility can be enhanced either by salt formation or by cocrystal formation. The ETZ molecule does not have any ionization site for salt formation; therefore, improvement in the solubility of ETZ drug molecule can only be done by cocrystallization. The solubility of ETZ and ETA·2TMA·MeOH in 37°C water was determined. The results in Fig. 5 clearly show that the solubility of ETA·2TMA·MeOH decreased to 19.30% of pure ETZ.

4 Conclusions

ETA·2TMA·MeOH cocrystal was prepared by solution evaporation crystallization, and the cocrystal was characterized by SCXRD, PXRD and FT-IR. It was proved that 1 molecule ETZ, 2 molecule TMA and 1 molecule MeOH formed cocrystal by hydrogen bonding. The synthesis of the new cocrystal was confirmed by Fourier Transform Infrared and Powder X-ray Diffraction. The crystal structure of the ETA·2TMA·MeOH crystal was characterized by Single Crystal X-ray Diffractometer. In addition, the influence of cocrystallization on the solubility of ETZ was determined by HPLC. The results showed that the solubility of ETA·2TMA·MeOH decreased to 19.30% of pure ETZ. Its pharmacological and toxicological properties need further study.

Declarations

Data Availability Statement

The datasets generated during and/or analysed during the current study are not publicly available due [REASON(S) WHY DATA ARE NOT PUBLIC] but are available from the corresponding author on reasonable request.].

Conflict of Interest Statement

I declare that the authors have no competing interests as defined by Springer, or other interests that might be perceived to influence the results and/or discussion reported in this paper.

References

1. Ozawa M, Hasegawa K, Yonezawa Y, Sunada H (2002) Preparation of solid dispersion for ethenzamide-carbopol and theophylline-carbopol systems using a twin screw extruder. Chemical and pharmaceutical bulletin 50(6): 802-807. https://doi.org/10.1248/cpb.50.802
2. Aitipamula S, Chow P S, Tan R B H (2010) Conformational and enantiotropic polymorphism of a 1: 1 cocrystal involving ethenzamide and ethylmalonic acid. CrystEngComm 12(11): 3691-3697. https://doi.org/10.1039/C004491A
3. Acebedo-Martínez F J, Alarcón-Payer C, Rodríguez-Domingo L, Domínguez-Martín A, Gómez-Morales J (2021) Furosemide/non-steroidal anti-inflammatory drug-drug pharmaceutical solids: Novel opportunities in drug formulation. Crystals, 11(11): 1339.https://doi.org/10.3390/cryst11111339
4. Nechipadappu, S K, Trivedi D R (2018) Cocrystal of nutraceutical sinapic acid with Active Pharmaceutical Ingredients ethenzamide and 2-chloro-4-Nitrobenzoic acid: Equilibrium solubility and stability study. Journal of Molecular Structure 1171: 898-905. https://doi.org/10.1016/j.molstruc.2018.06.074
5. Khatioda R, Saikia B, Das P J, Sarma B (2017) Solubility and in vitro drug permeation behavior of ethenzamide cocrystals regulated in physiological pH environments. CrystEngComm 19(46): 6992-7000. https://doi.org/10.1039/C7CE01626C
6. Potticary J, Hall C, Hamilton V, Hamilton V, McCabe J F, Hall S R (2020) Crystallization from volatile deep eutectic solvents. Crystal Growth & Design 20(5): 2877-2884. https://doi.org/10.1021/acs.cgd.0c00399
7. Aitipamula S, Chow P S, Tan R B H. Polymorphs and solvates of a cocrystal involving an analgesic drug, ethenzamide, and 3, 5-dinitrobenzoic acid[J]. Crystal growth & design, 2010, 10(5): 2229-2238. https://doi.org/10.1021/cg9015178
8. Khatioda R, Bora P, Sarma B (2018) Trimorphic ethenzamide cocrystal: in vitro solubility and membrane efflux studies. Crystal Growth & Design 18(8): 4637-4645. https://doi.org/10.1021/acs.cgd.8b00603
9. Hariprasad V M, Nechipadappu S K, Trivedi D R (2016) Cocrystals of ethenzamide: study of structural and physicochemical properties. Crystal Growth & Design 16(8): 4473-4481. https://doi.org/10.1021/acs.cgd.6b00606
10. Aitipamula S, Wong A B H, Chow P S, Tan R B (2012) Pharmaceutical cocrystals of ethenzamide: structural, solubility and dissolution studies. CrystEngComm 14(24): 8515-8524. https://doi.org/10.1039/C2CE26325D

11. Kozak A, Marek P H, Pindelska E (2019) Structural characterization and pharmaceutical properties of three novel cocrystals of ethenzamide with aliphatic dicarboxylic acids. Journal of pharmaceutical sciences 108(4): 1476-1485. https://doi.org/10.1016/j.xphs.2018.10.060
12. Nechipadappu S K, Tekuri V, Trivedi D R (2017) Pharmaceutical co-crystal of flufenamic acid: synthesis and characterization of two novel drug-drug co-crystal. Journal of Pharmaceutical Sciences 106(5): 1384-1390. https://doi.org/10.1016/j.xphs.2017.01.033
13. Sarmah K K, Boro K, Arhangelskis M, Thakuriaet R (2017) Crystal structure landscape of ethenzamide: a physicochemical property study. CrystEngComm 19(5): 826-833. https://doi.org/10.1039/C6CE02057G
14. Kozak A, Marek P H, Pindelska E (2019) Structural characterization and pharmaceutical properties of three novel cocrystals of ethenzamide with aliphatic dicarboxylic acids. Journal of pharmaceutical sciences 108(4): 1476-1485. https://doi.org/10.1016/j.xphs.2018.10.060
15. Aitipamula S, Chow P S, Tan R B H (2010) Conformational and enantiotropic polymorphism of a 1: 1 cocrystal involving ethenzamide and ethylmalonic acid. CrystEngComm 12(11): 3691-3697. https://doi.org/10.1039/C004491A
16. Aitipamula S, Chow P S, Tan R B H (2009) Dimorphs of a 1: 1 cocrystal of ethenzamide and saccharin: solid-state grinding methods result in metastable polymorph. CrystEngComm 11(5): 889-895.https://doi.org/10.1039/B821373A

Figures

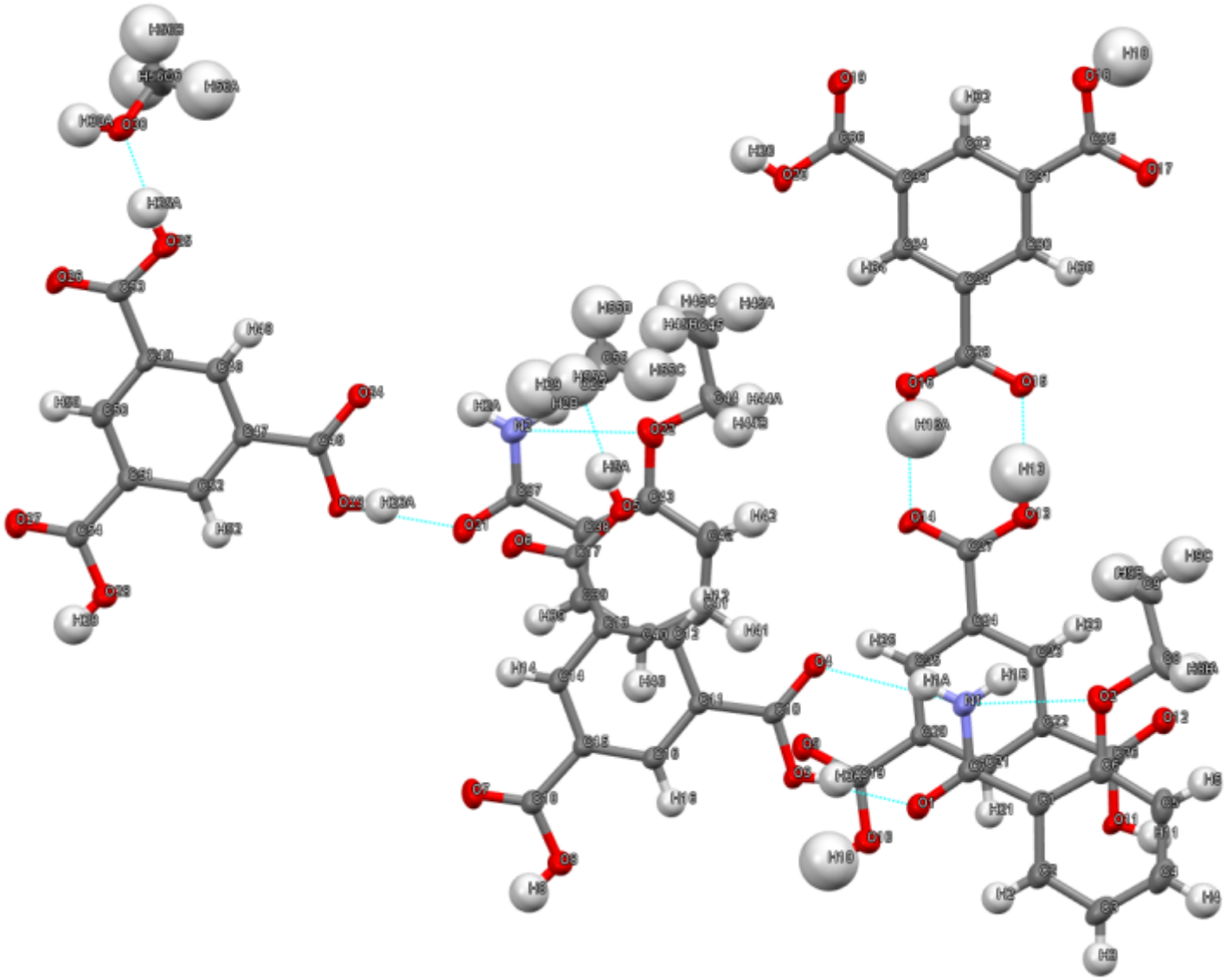

Figure 1

Cocrystallization of ETA·2TMA·MeOH

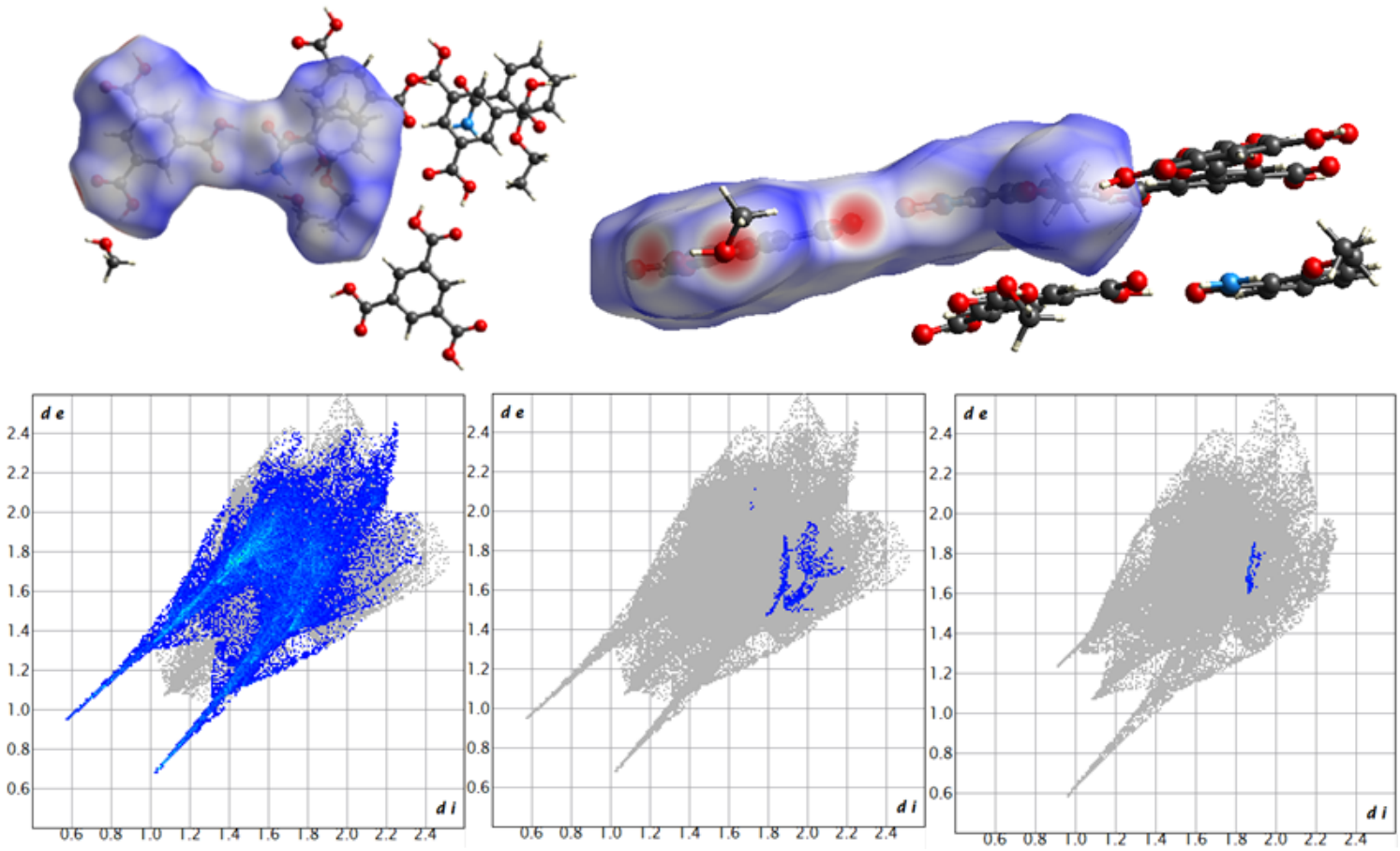

Figure 2

Views of the calculated ETA·2TMA·MeOH Hirshfeld surface

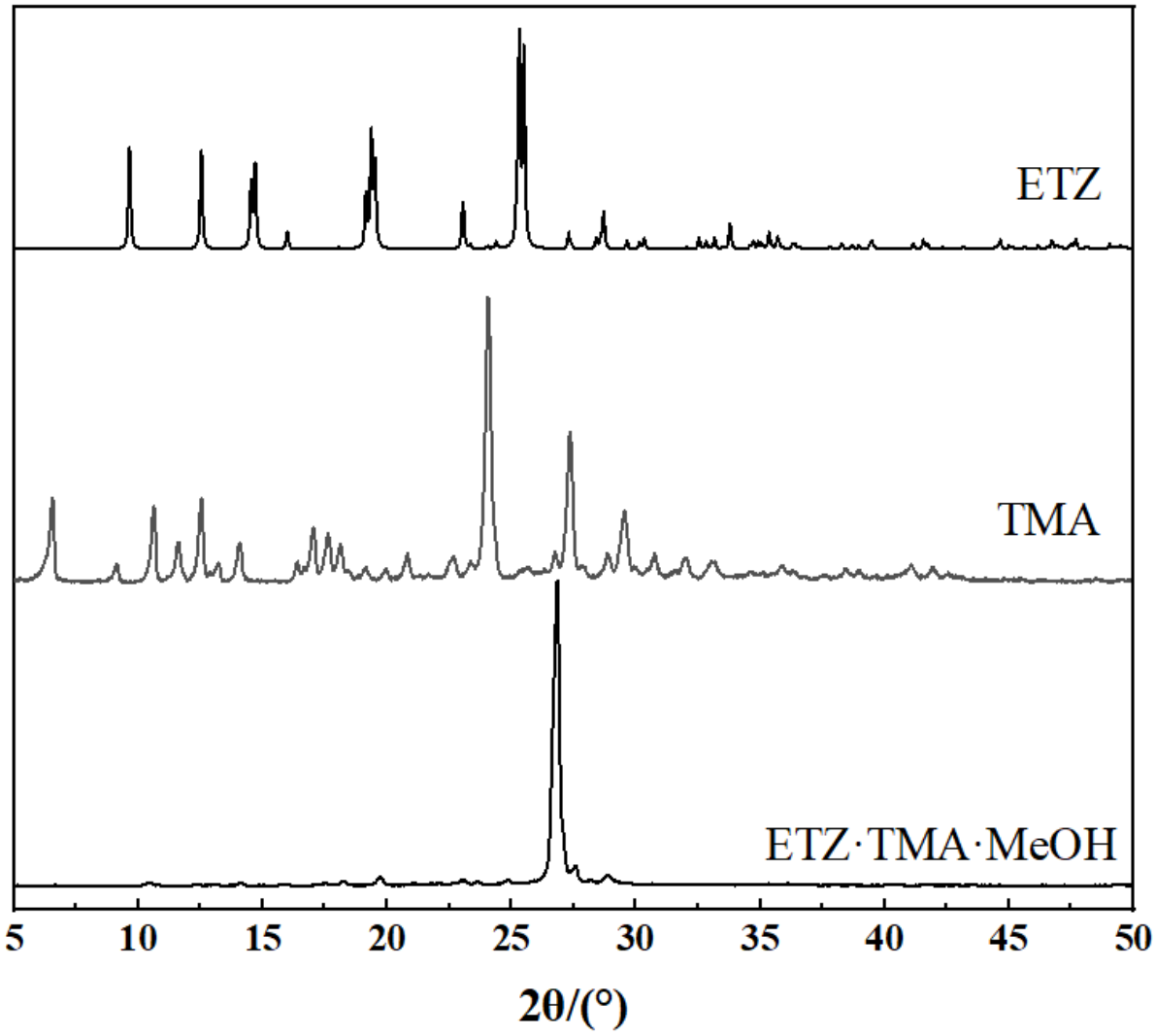

Figure 3

The powder X-ray diffraction (PXRD) patterns of ETZ, TMA and ETA·2TMA·MeOH

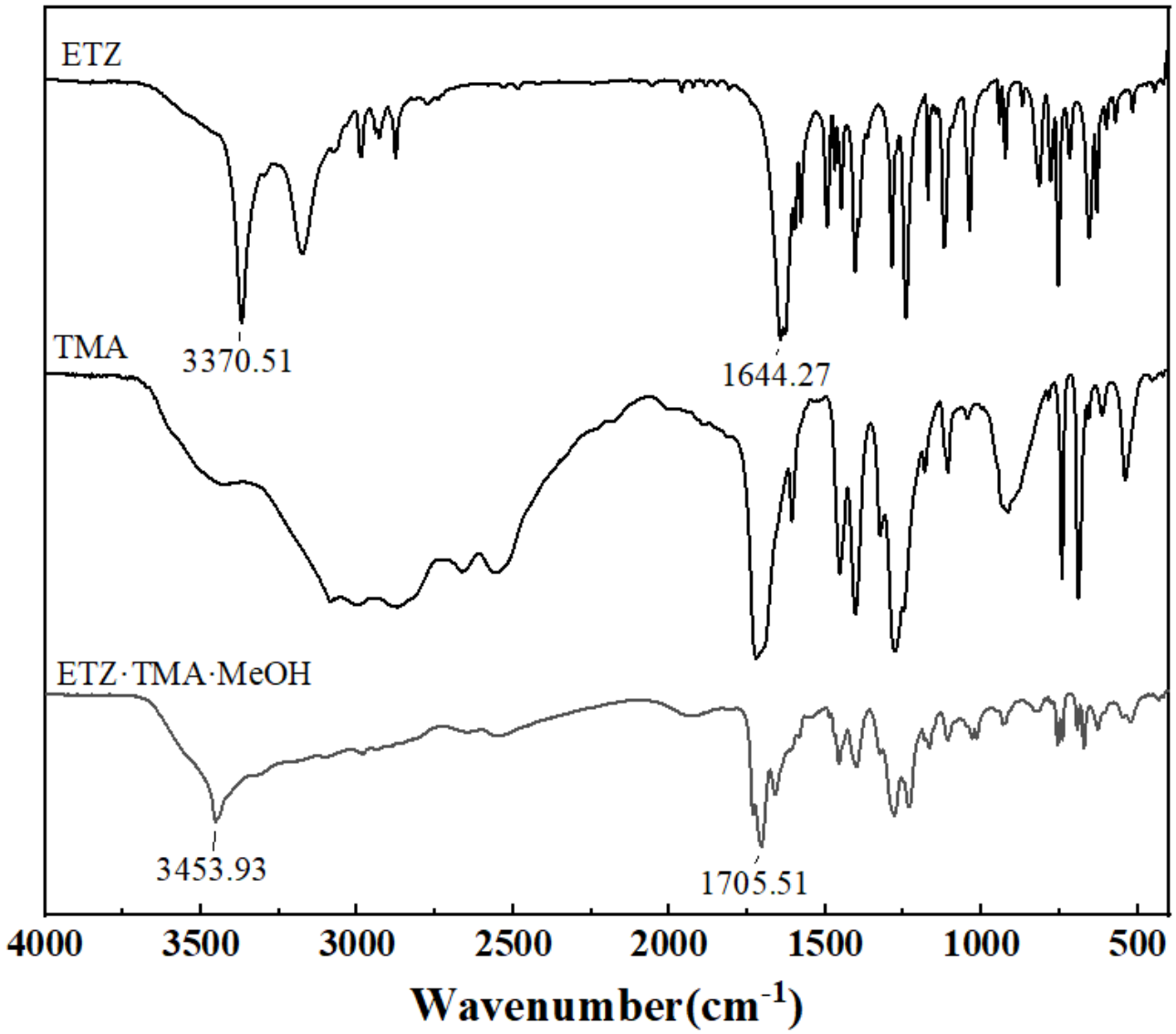

Figure 4

Comparison of FT-IR spectra of ETZ TMA and ETA·2TMA·MeOH

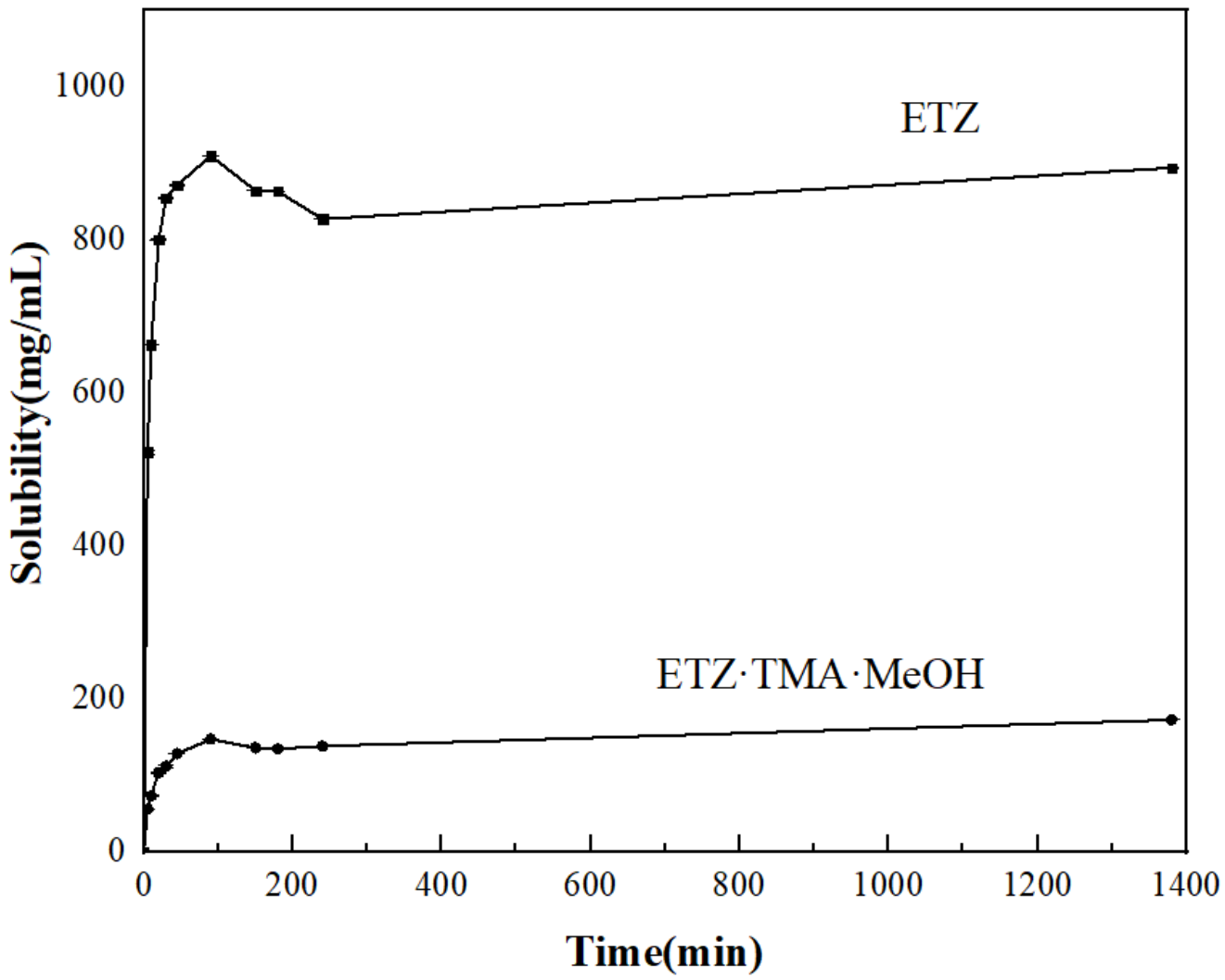

Figure 5

Solubility of ETZ and ETA·2TMA·MeOH in aqueous solution

Supplementary Files

This is a list of supplementary files associated with this preprint. Click to download.

- GraphicalAbstract.png